Parameters of Fe/Cr interfacial electron scattering from infrared magnetoreflection

I. D. Lobov, M. M. Kirillova, A. A. Makhnev, L. N. Romashev, and V. V. Ustinov
Institute of Metal Physics, Ural Division, Russian Academy of Sciences, 620041 Ekaterinburg, Russia
(Received 28 October 2009; revised manuscript received 9 April 2010; published 29 April 2010)

The magnetorefractive effect is studied in the infrared spectral region of 2–13 μm in molecular-beam epitaxy-grown $[\mathrm{Fe}(t_{\mathrm{Fe}},\ \text{Å})/\mathrm{Cr}(10\ \text{Å})]_n$ superlattices. The Fe layer thickness varies from 15.3 to 7.2 Å. The effective dielectric function $\varepsilon_{\mathrm{eff}}$ and the giant magnetoresistance were measured on the same samples. Relaxation times $\tau_i^{\uparrow(\downarrow)}$ and scattering probabilities $P_i^{\uparrow(\downarrow)}$ of conduction electrons at interfaces, as well as spin asymmetry coefficient $\gamma_{\mathrm{Fe/Cr(100)}}$ were obtained from the magnetoreflection in the intraband absorption region. The experimental estimations of the scattering parameters of conduction electrons are compared with the available results of theoretical calculations.

DOI: 10.1103/PhysRevB.81.134436 PACS number(s): 78.20.Ls, 78.20.Ci, 75.47.−m, 73.50.−h

I. INTRODUCTION

Giant magnetoresistance (GMR) in multilayer and granular structures is related to the asymmetry of spin-dependent scattering of conduction electrons at interfaces and in ferromagnetic layers.[1–5] For the first time the magneto-optical response of a new kind referred to as magnetorefractive effect (MRE) was experimentally detected and theoretically described at magnetotransmission in $\mathrm{Ni_{80}Fe_{20}/Cu/Co/Cu}$ multilayer structure.[6] Nongyrotropic (an even function of magnetization) MRE characterizes the effect of an applied magnetic field on a complex refractive index $\tilde{n}$ ($\tilde{n}^2=\varepsilon$, ε is a dielectric constant) and, respectively, on the reflection and transmission coefficients. In an intraband absorption region, the MRE is caused by the asymmetry of conduction electrons scattering for up-spin ($\uparrow$) and down-spin ($\downarrow$) directions relative to spontaneous magnetization in the bulk and at interfaces of ferromagnetic layers, and therefore the MRE is often called high-frequency (optical) analog of the GMR. By present time, MRE was theoretically developed[7–10] and experimentally observed[11–16] in a wide variety of materials. Several MRE investigations of Fe/Cr system are available.[17–19] However, all of them gave a sign opposite to that expected from the intraband (Drude) absorption and only recently the correct sign of the MRE was obtained.[20]

It is known that low-energy interband excitations of electrons arise in transition *d* metals. Therefore one should study an effect of interband transitions on the magnitude and sign of the magnetoreflection in Fe/Cr system. The interfacial scattering of conduction electrons plays the key role in magnetotransport properties of GMR systems and its characterization is very urgent. So, the main objective of this work was to determine scattering parameters for both up-spin and down-spin conduction electrons at the Fe/Cr(100) interface. The paper is organized as follows: in Sec. II the details concerning sample preparation and the experimental methods are presented. Section III A is devoted to optical and electronic characteristics of the Fe/Cr superlattices. Section III B provides the description of the magnetorefractive experiment and the comparison of GMR and MRE data. The parameters of conduction electrons responsible for magnetotransport properties are obtained in Sec. III C and we briefly summarize our paper in Sec. IV.

II. EXPERIMENTAL METHODS

In this paper we measured optical absorption, MRE, and GMR. Optical measurements were carried out in the infrared (IR) range of spectra where Drude-type absorption of light is traditionally considered dominating in metals. We studied a set of $(100)\mathrm{MgO/Cr}(80\ \text{Å})/[\mathrm{Fe}(t_{\mathrm{Fe}},\ \text{Å})/\mathrm{Cr}(10\ \text{Å})]_{30}$ superlattices ($t_{\mathrm{Fe}}=7.2$–15.3 Å), grown in ultrahigh vacuum by the molecular-beam epitaxy technique. The Cr layers thickness was equal to 10 Å which ensured the giant magnetoresistance and antiferromagnetic ordering of magnetic moments of the adjacent Fe layers in the absence of external magnetic field. The superlattice period and layer thickness were determined from the low-angle x-ray diffraction spectra, deposition rate, and time. The layer thicknesses in superlattices are small in comparison with the classical skin depth in bulk Fe and Cr ($\delta_0=c/\omega k$,where *c* is the velocity of light in vacuum, ω is a cyclic frequency of light, and *k* is an absorption coefficient). Both Fe and Cr dielectric functions are high enough ($\varepsilon_{\mathrm{Fe}},\varepsilon_{\mathrm{Cr}}\gg 1$), so we can consider a superlattice as an effective medium and use $\varepsilon_{\mathrm{eff}}$ for its description. Label "eff" will be omitted at further discussion of optical characteristics. The effective optical constants *n* and *k* were measured by the ellipsometric method[21] in the spectral region of 0.3–13 μm at angles of light incidence of 76°–82°. The measurement error of optical constants *n* and *k* did not exceed 5%. From *n* and *k* the real $\varepsilon_1(\omega)=n^2-k^2$ and imaginary $\varepsilon_2(\omega)=2nk$ parts of the effective dielectric function $\varepsilon(\omega)$ and the optical conductivity $\sigma(\omega)=nk\omega/2\pi$ were defined. MRE is defined as

$$\mathrm{MRE}=[R(0)-R(H)]/R(0), \tag{1}$$

where $R(0)$ and $R(H)$ are the reflectivities of a sample in nonmagnetized state ($H=0$) and in an applied magnetic field ($H\neq 0$), respectively. The change in the reflectivity in an applied magnetic field reaches maximum when magnetization ordering of adjacent magnetic layers changes from antiferromagnetic to ferromagnetic. The effect has the negative sign in the free carriers region due to an increase in real part of conductivity at ferromagnetic ordering of the magnetic moments of layers in an applied magnetic field, $R(\omega,H=0)<R(\omega,H\neq 0)$. The MRE infrared reflection spectra were measured in transverse geometry in *p*- and

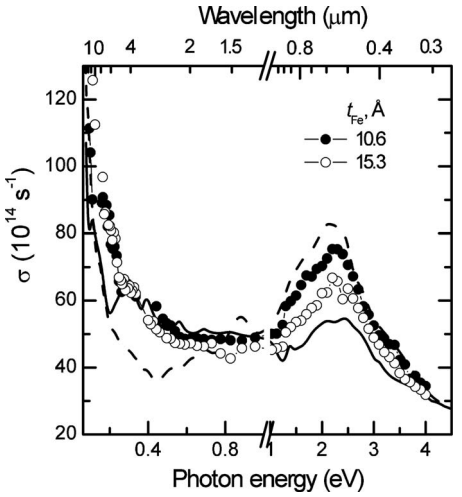

FIG. 1. Spectra of optical conductivity of Fe/Cr superlattices. Fe thickness: empty circles—15.3 Å; full circles—10.6 Å. Solid (dashed) line represents optical conductivitiy of bulk Fe(Cr), respectively.

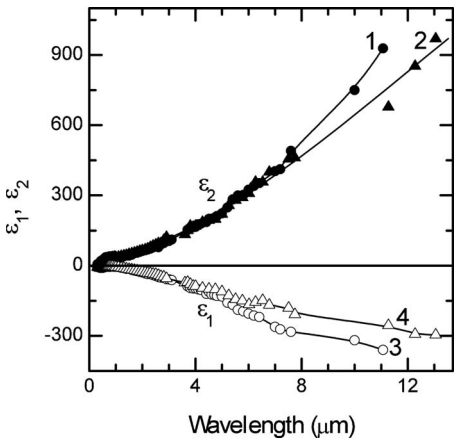

FIG. 2. Dielectric functions ε_1 and ε_2 of Fe/Cr superlattices. Fe layer thickness: 1,3—15.3 Å; 2,4—10.6 Å. Lines are guide for eye.

s-polarized light using IR spectrometer with optoacoustic detector and grid polarizer. The angle of incidence for *p* (*s*) polarization of light was set at 70° (10°) with respect to the surface normal. The spectral region was between 2 and 13 μm. To magnetize a sample a compact shielded electromagnet with electric current in a form of unipolar meander was used. Dynamic magnetization reversal was performed with frequency of 8 Hz, magnetic field varied from 0 to 9 kOe. The magnetoresistance was measured in a magnetic field of $H \leq 32$ kOe by a standard four-contact method in CIP geometry. The magnetoresistance is defined as

$$r = [\rho(H) - \rho(0)]/\rho(0), \tag{2}$$

where $\rho(0)$ and $\rho(H)$ are the resistances in nonmagnetized state and in the magnetic field H, respectively. All measurements were carried out at room temperature.

III. DISCUSSION

A. Optical and electronic characteristics

The results of optical study $[\sigma(\omega), \varepsilon_1(\lambda), \varepsilon_2(\lambda)]$ for two samples are presented in Figs. 1 and 2. Optical conductivities for Fe (Ref. 22) and Cr (Ref. 23) are given for comparison, Fig. 1. Low-energy interband absorption in IR range of $\hbar\omega = 0.15-0.53$ eV ($\lambda = 2.3-8.2$ μm) is the specific feature of the optical properties of Fe.[22] Theoretical analysis of optical data showed that the anomaly of optical absorption is caused by electron transitions of $(d,p\text{-}p,d)$ type in spin-down bands $E(\mathbf{k})$ and also by hybridization of bands with opposite spin direction nearby the Fermi level due to spin-orbit interaction.[24,25] Thus, the significant interband contribution to optical conductivity of Fe in the spectral region of 2–8 μm was observed experimentally and got theoretical explanation. Interband absorption in the mentioned wavelength interval is observed in Fe/Cr superlattices as well (Fig. 1).

The behavior of dielectric functions $\varepsilon_1(\lambda)$ and $\varepsilon_2(\lambda)$ testifies to a dominating contribution to optical conductivity of the Drude absorption at $\lambda > 8$ μm, Fig. 2. The analysis of frequency dependences of $\varepsilon_1(\lambda)$ and $\varepsilon_2(\lambda)$ makes it possible to estimate the effective plasma frequency ω_p and effective relaxation time τ^{opt} of conduction electrons. These parameters are presented in Table I. Here, N_{eff} is the effective concentration of conduction electrons defined as $(\omega_p)^2 = 4\pi N_{eff} e^2/m_0$ (e and m_0 denote the charge and mass of a free electron, respectively). The values of ω_p are used further in simulation of the MRE spectra and the values of τ^{opt} are compared with the relaxation time of conduction electrons defined from the magnetorefractive data.

B. Correlation between MRE and GMR

The MRE spectra in *p*-polarized light for three superlattices are shown in Fig. 3. The effect has an alternating quantity being positive in the near-infrared region and becoming negative in the region of $\lambda > 5.3$ μm (for $t_{Fe} = 15.3$ Å), $\lambda > 6.3$ μm (for $t_{Fe} = 10.6$ Å), and $\lambda > 6.8$ μm (for $t_{Fe} = 7.2$ Å). The study of the optical conductivity and dielectric function results in conclusion that the region of the positive values of MRE is caused by low-energy interband transitions of electrons. Recently, Baxter *et al.*[26] calculated MRE for Co/Cu in the tight-binding approximation and showed that interband transitions can result in the positive sign of MRE. The separation of intraband and interband contribu-

TABLE I. Parameters of conduction electrons from optical ellipsometry: plasma frequency $\hbar\omega_p$, effective concentration N_{eff}, and effective relaxation time τ_{eff}^{opt}.

t_{Fe} (Å)	$\hbar\omega_p$ (eV)	N_{eff} (10^{28} m^{-3})	τ_{eff}^{opt} (10^{-15} s)
7.2	3.22	0.76	3.3
10.6	3.30	0.79	3.8
15.3	3.35	0.82	4.3

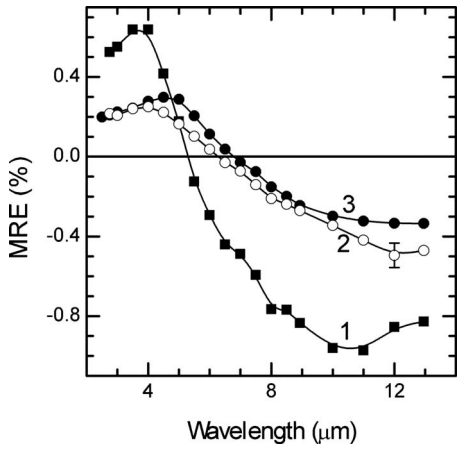

FIG. 3. Experimental MRE spectra in *p*-polarized IR light for Fe/Cr superlattices in an applied field of 9 kOe. Fe thickness: 1—15.3 Å; 2—10.6 Å; 3—7.2 Å. Vertical segment specifies measurement error.

tions to MRE spectrum are made in the following section for Fe(10.6 Å)/Cr(10 Å) sample. The maximum negative MRE values of our samples in *p*-polarized light at the angle of incidence of $\varphi=70°$ in an applied magnetic field of 9 kOe are equal to: (−1%) for $[\text{Fe}(15.3\ \text{Å})/\text{Cr}(10\ \text{Å})]_{30}$, (−0.50%) for $[\text{Fe}(10.6\ \text{Å})/\text{Cr}(10\ \text{Å})]_{30}$, and (−0.34%) for $[\text{Fe}(7.2\ \text{Å})/\text{Cr}(10\ \text{Å})]_{30}$. The MRE magnitude in *s*-polarized light is two to three times smaller.

The magnetoresistance of the samples as a function of an applied magnetic field is shown in Fig. 4. The maximum GMR value is observed in a saturating magnetic field in the sample with $t_{\text{Fe}}=10.6$ Å while in a 9 kOe magnetic field the maximum GMR value is found in the sample with $t_{\text{Fe}}=15.3$ Å. Figure 5 represents experimental GMR and MRE data as functions of the applied magnetic field in the expanded scale. Magnetic field dependences of MRE are measured at 9.5 μm in the intraband part [Figs. 5(a)–5(c)] and at 4 μm in the interband part of the spectrum, Fig. 5(d). Correlation between MRE and GMR is observed in both ranges of the spectrum though MRE at 4 μm has an opposite sign. A small contribution from linear magneto-optical effects to MRE is displayed as an insignificant offset of the plot, Fig. 5(d).

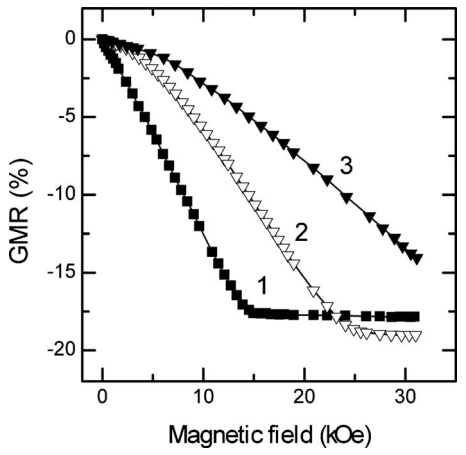

FIG. 4. Experimental GMR data of Fe/Cr superlattices: 1—$[\text{Fe}(15.3\ \text{Å})/\text{Cr}(10\ \text{Å})]_{30}$; 2—$[\text{Fe}(10.6\ \text{Å})/\text{Cr}(10\ \text{Å})]_{30}$; 3—$[\text{Fe}(7.2\ \text{Å})/\text{Cr}(10\ \text{Å})]_{30}$.

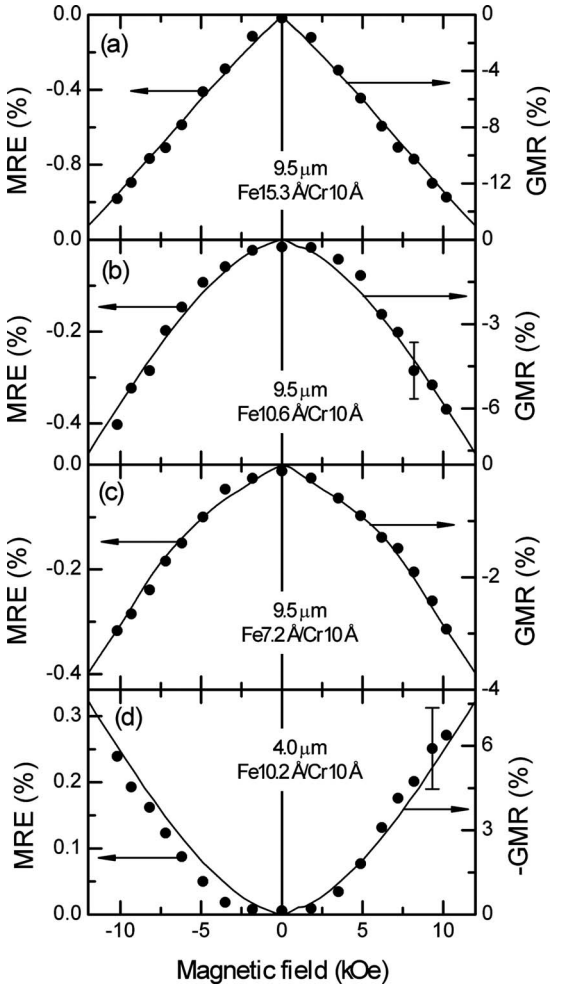

FIG. 5. Correlation between experimental GMR data and experimental MRE values shown as a function of an applied magnetic field. Vertical segment specifies measurement error.

At the maximum value of MRE ($\lambda=11$ μm), $\text{GMR}/\text{MRE}^{\text{P}}$ in Fe(15.3 Å)/Cr(10 Å) sample is approximately equal to 12. According to the available representations,[27] the MRE magnitude is to rise with the increase in the wavelength up to the Hagen-Rubens region $[\omega\tau\ll 1, n\sim k, R(\varphi=0^o)\approx 1-2(\omega/2\pi\sigma)^{1/2}]$ and then tend to zero as $\omega^{1/2}$. The electronic characteristics obtained from the optical data show that the Hagen-Rubens region is not reached for our samples since the relation $\omega\tau^{\text{opt}}\ll 1$ is not strictly fulfilled for all of them in the spectral range explored. The condition is slightly improved for the sample with $t_{\text{Fe}}=7.2$ Å due to the decrease in the effective relaxation time τ^{opt} by ~23% (Table I). At the maximum magnitude of MRE (13 μm), the $\text{GMR}/\text{MRE}^{\text{P}}$ ratio is approximately equal to 7.5 for this sample.

C. MRE spectra simulation

Simulation of the MRE spectra is performed within the Jacquet-Valet (JV) theory[6] for multilayer structures, where

the real and imaginary parts of the modified complex Drude dielectric function $\varepsilon_{\mathrm{SAL}}$ are

$$\mathrm{Re}\ \varepsilon_{\mathrm{SAL}} = \varepsilon_{st} - \frac{\omega_p^2 \tau_{\mathrm{SAL}}^2 (1 + \omega^2 \tau_{\mathrm{SAL}}^2 + m^2 \beta_{\mathrm{SAL}}^2)}{(1 - \omega^2 \tau_{\mathrm{SAL}}^2 - m^2 \beta_{\mathrm{SAL}}^2)^2 + 4\omega^2 \tau_{\mathrm{SAL}}^2}, \quad (3)$$

$$\mathrm{Im}\ \varepsilon_{\mathrm{SAL}} = - \frac{\omega_p^2 \tau_{\mathrm{SAL}} (1 + \omega^2 \tau_{\mathrm{SAL}}^2 - m^2 \beta_{\mathrm{SAL}}^2)}{\omega[(1 - \omega^2 \tau_{\mathrm{SAL}}^2 - m^2 \beta_{\mathrm{SAL}}^2)^2 + 4\omega^2 \tau_{\mathrm{SAL}}^2]}. \quad (4)$$

There ε_{st} is the frequency independent contribution to $\varepsilon_{\mathrm{SAL}}$, ω_p is the plasma frequency of conduction electrons, and m is the parameter characterizing relative magnetization of layers ($m=M/M_s$, M_s is the saturation magnetization). The average relaxation time of conduction electrons τ_{SAL} in a zero field and the parameter of average spin asymmetry β_{SAL} are obtained in the self-averaging limit[6] (SAL) of probabilities of electron scattering over a period of a multilayer structure $T = t_{\mathrm{Fe}} + t_{\mathrm{Cr}} + 2t_i$, where t_i is the thickness of the interface layer. The probability of an electron scattering P at passing of one period of superlattice T defines the effective relaxation rate of electrons τ_{SAL}^{-1}

$$\frac{1}{\tau_{\mathrm{SAL}}} = \frac{\langle \nu_{\mathrm{F}} \rangle}{T} P, \quad (5)$$

where $\langle \nu_{\mathrm{F}} \rangle$ is the average electron velocity on the Fermi surface (assuming $\langle \nu_{\mathrm{F}} \rangle_{\mathrm{Fe}} \approx \langle \nu_{\mathrm{F}} \rangle_{\mathrm{Cr}} = \langle \nu_{\mathrm{F}} \rangle$). Probability P is the sum of scattering probabilities of an electron in Fe (P_{Fe}) and Cr (P_{Cr}) layers, and at two interfaces ($2P_i$): $P = P_{\mathrm{Fe}} + P_{\mathrm{Cr}} + 2P_i$. The value of P_i is assumed to be the same for Fe/Cr and Cr/Fe interfaces. For convenience of simulation τ_{SAL} and β_{SAL} are represented according to Vopsaroiu *et al.*[13] as $(\tau_{\mathrm{SAL}})^{-1} = 2c_i/\tau_i + c_{\mathrm{Fe}}/\tau_{\mathrm{Fe}} + (1 - 2c_i - c_{\mathrm{Fe}})/\tau_{\mathrm{Cr}}$ and $\beta_{\mathrm{SAL}} = \tau_{\mathrm{SAL}} \times (\gamma(2c_i)/\tau_i + \beta c_{\mathrm{Fe}}/\tau_{\mathrm{Fe}})$. Here, c_{Fe} and c_i are the volume fractions of Fe and interface layers; τ_i, τ_{Fe}, and τ_{Cr} are the effective relaxation times of conduction electrons at interfaces, in Fe, and Cr layers, respectively; γ and β are the coefficients of spin asymmetry at an interface and in Fe layer. We also assume the absence of spin-dependent scattering in Cr layers. It should be noted that γ and β were introduced in the two-current model of magnetoresistance[28] and there are only theoretical estimations of the indicated parameters for Fe/Cr structures. Using the Fresnel formulas for complex reflection coefficients $r^{s,p}$

$$r^s = \frac{\cos\varphi - (\varepsilon - \sin^2\varphi)^{1/2}}{\cos\varphi + (\varepsilon - \sin^2\varphi)^{1/2}}, \quad (6)$$

$$r^p = \frac{\varepsilon \cos\varphi - (\varepsilon - \sin^2\varphi)^{1/2}}{\varepsilon \cos\varphi + (\varepsilon - \sin^2\varphi)^{1/2}}, \quad (7)$$

where $\varepsilon = \varepsilon_{\mathrm{SAL}}(\omega, H)$ and φ is an angle of incidence, it is possible to express the intensity of the reflected s- and p-polarized light as

$$|r^s|^2 = \frac{\cos^2\varphi + A - \sqrt{2}\cos(\varphi)\sqrt{A+B}}{\cos^2\varphi + A + \sqrt{2}\cos(\varphi)\sqrt{A+B}}, \quad (8)$$

$$|r^p|^2 = \frac{|\varepsilon|^2 \cos^2\varphi + A - \sqrt{2}\cos(\varphi)C}{|\varepsilon|^2 \cos^2\varphi + A + \sqrt{2}\cos(\varphi)C}, \quad (9)$$

where $A = \sqrt{[\mathrm{Re}(\varepsilon) - \sin^2\varphi]^2 + \mathrm{Im}(\varepsilon^2)}$, $B = \mathrm{Re}(\varepsilon) - \sin^2\varphi$, $C = \mathrm{Re}(\varepsilon)\sqrt{A+B} + \mathrm{Im}(\varepsilon)\sqrt{A-B}$, and to define the MRE value by Eq. (1).

At MRE simulation the number of arbitrarily varied parameters should be reduced as much as possible. The plasma frequency ω_p was defined from the optical measurements in the IR region (see Table I). We took the values of relaxation time of conduction electrons from the optical measurements[22,23] in the IR region for bulk Fe and Cr ($\tau_{\mathrm{Cr}} = \tau_{\mathrm{Fe}} \simeq 1.2 \times 10^{-14}$ s). We accepted the values of $m(H=9$ kOe) equal to 0.818, 0.514, and 0.391 (Ref. 29) for the samples with $t_{\mathrm{Fe}} = 15.3$ Å, 10.6 Å, and 7.2 Å, respectively. Contributions to the interfacial layer from Fe and Cr layers are assumed to be the same and the interface thickness t_i is assumed to be 2.88 Å (two monolayers). The spin asymmetry coefficient γ and the relaxation time τ_i are assumed to be independent on thickness of Fe and Cr layers since the samples were prepared in identical conditions, and pure Fe and Cr layers are still left after interface formation. In particular, under such a choice of interface thickness, three Fe monolayers are still left even in the sample with $t_{\mathrm{Fe}} = 7.2$ Å. The ironlike spectrum of transverse Kerr effect for Fe(7.2 Å)/Cr(10 Å) sample confirms this assumption.[30] The spin asymmetry coefficient β of a ferromagnetic layer was taken from the density-of-states ratio of Fe (Ref. 31) at the Fermi level ($n_{\mathrm{F}}^{\downarrow}/n_{\mathrm{F}}^{\uparrow} = 0.27$), $\beta = (n_{\mathrm{F}}^{\uparrow} - n_{\mathrm{F}}^{\downarrow})/(n_{\mathrm{F}}^{\uparrow} + n_{\mathrm{F}}^{\downarrow}) \simeq 0.57$. Thus, we reduced an arbitrary choice of parameters for the numerical simulation of MRE spectra to γ and τ_i determination.

Satisfactory agreement of the calculated data with the maximal experimental $\mathrm{MRE}^{\mathrm{P}}$ values in the region of free carriers was reached by variation in τ_i and γ. We also took into account the negative sign of $\gamma_{\mathrm{Fe/Cr}}$ obtained both from experimental study of GMR inversion[32] and from the first-principles calculations.[33] The negative sign of the spin asymmetry coefficient of the Fe/Cr(100) interface indicates a higher conductivity of spin-down ($\downarrow$) current channel and is explained by the close fit of the energy bands $E(\mathbf{k})$ ($\downarrow$) of Fe and $E(\mathbf{k})$ of paramagnetic Cr. As a result, spin-down electrons are weaker scattered at an interface.

The results of MRE spectra simulation are given in Table II. The averaged value of γ, $\gamma_{\mathrm{Fe/Cr(100)}} = -0.59 \pm 0.04$, is in close agreement with theoretical estimation of this parameter (Table II). The averaged value of τ_i is equal to $(1.79 \pm 0.16) \times 10^{-15}$ s. Calculated from $\tau_i^{\uparrow\downarrow} = \tau_i/(1 \mp \gamma m)$, the relaxation times of conduction electrons for spin-up and spin-down subbands at the Fe/Cr(100) interface have the following values for $m=1$: $\tau_i^{\uparrow} = 1.13 \times 10^{-15}$ s and $\tau_i^{\downarrow} = 4.37 \times 10^{-15}$ s. The probability of electron scattering at an interface for up-spin and down-spin directions can be estimated from $P_i^{\uparrow(\downarrow)} = t_i/(\tau_i^{\uparrow(\downarrow)} \langle \nu_F^{\uparrow(\downarrow)} \rangle)$. From the angle-resolved photoemission on Fe (Ref. 34) one can estimate $\nu_{\mathrm{F}}^{\uparrow(\downarrow)}$ in [100] direction: $\langle \nu_{\mathrm{F}}^{\uparrow} \rangle \approx 10.8 \times 10^7$ cm/s and $\langle \nu_{\mathrm{F}}^{\downarrow} \rangle \approx 6.7 \times 10^7$ cm/s. Thus, we obtained the probabilities of electron scattering at an interface: $P_i^{\uparrow} = 0.24$ and $P_i^{\downarrow} = 0.10$.

TABLE II. Parameters of conduction electrons from magnetoreflection. Interface parameters: spin asymmetry coefficient γ; relaxation time τ_i. Superlattice parametrs: average spin asymmetry constant β_{SAL}; average relaxation time τ_{SAL}.

	Interface		Superlattice	
t_{Fe} (Å)	γ	τ_i (10^{-15} s)	β_{SAL}	τ_{SAL} (10^{-15} s)
7.2	−0.55	1.95	−0.36	4.4
10.6	−0.58	1.74	−0.34	4.5
15.3	−0.63	1.63	−0.32	4.9
	−0.58[a]			

[a]Reference 33.

Then we estimated the mean-free path of conduction electrons $l^{\uparrow(\downarrow)}=\langle v_F^{\uparrow(\downarrow)}\rangle \tau_{SAL}^{\uparrow(\downarrow)}$ in the Fe(10.6 Å)/Cr(10 Å) sample. From $\tau_{SAL}^{\uparrow(\downarrow)}=\tau_{SAL}/(1\mp m\beta_{SAL})$ for $m=1$ we get $\tau_{SAL}^{\uparrow}=3.4\times10^{-15}$ s and $\tau_{SAL}^{\downarrow}=6.9\times10^{-15}$ s. Using these values and the above given $\langle v_F^{\uparrow(\downarrow)}\rangle$, we get $l^{\uparrow}=37$ Å and $l^{\downarrow}=46$ Å which satisfy the requirements of SAL formalism. Besides, the values of the effective relaxation time τ^{opt} agree within the limits of 20% with the values of τ_{SAL} defined from MRE simulation.

The experimental and calculated MRE spectra of the $[Fe(10.6\ Å)/Cr(10\ Å)]_{30}$ superlattice are given in *s*- and *p*-polarized light in Fig. 6. The treatment of model curves 3 and 4 (Fig. 6) shows that the contribution to the effect from free carriers decreases to zero at the short wavelengths while it gradually rises with an increase in λ. Such behavior agrees with the frequency dispersion of dielectric functions (Fig. 2). The difference between the experimental and calculated MRE spectra at $\lambda<8$ μm consists in the interband contribution to magnetorefractive response (Fig. 6, curve 5). Samples with 15.3 and 7.2 Å thickness of Fe have similar correspondence between the model and experimental MRE spectra.

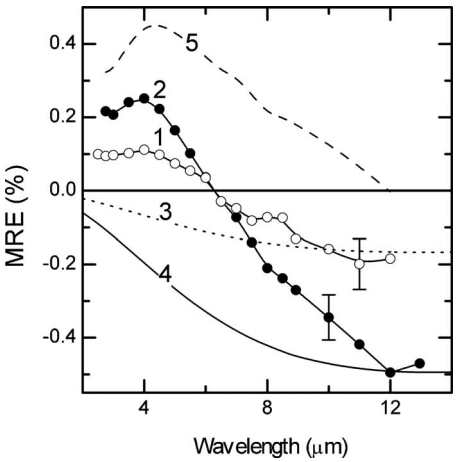

FIG. 6. MRE spectra of the Fe(10.6 Å)/Cr(10 Å) sample. 1(2)—experimental $MRE^{S(P)}$ spectra; 3(4)—model $MRE^{S(P)}$ spectra; 5—interband contribution to MRE^{P}. Parameters of simulation: $\hbar\omega_p=3.30$ eV; $M/M_s=0.514$; $\tau_{SAL}=4.5\times10^{-15}$ s; $\beta_{SAL}=-0.34$; $H=9$ kOe. Vertical segments specify measurement errors.

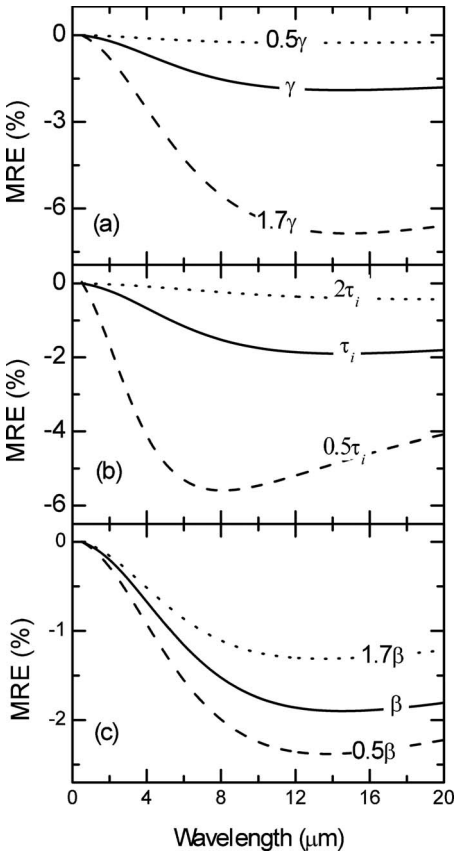

FIG. 7. Model MRE^{P} spectra for Fe(10.6 Å)/Cr(10 Å) sample calculated at $m=1$. Varying parameter: (a)—γ; (b)—τ_i; (c)—β.

For better understanding of MRE dependence on JV model parameters, we calculated the MRE spectra with a true set of parameters (from Table II) except the varied one for the $[Fe(10.6\ Å)/Cr(10\ Å)]_{30}$ superlattice. Figure 7 shows the results of such simulation for spin asymmetry coefficients β and γ, and the relaxation time at the interface τ_i (case $m=1$). As is seen from the plots, the MRE magnitude depends mainly on the interface parameters γ and τ_i. If the growth of γ increases mainly an amplitude of the effect, the decrease in τ_i results in considerable increase in MRE magnitude and in the shift of MRE maximum to the shorter wavelengths [Figs. 7(a) and 7(b)]. On the contrary, the growth of the spin asymmetry constant β of Fe layer leads only to the decrease in the effect owing to the opposite signs of β and γ (Fig. 7). Magnetoresistance in JV model is expressed as $r=-m^2\beta_{SAL}^2$. The value of GMR for Fe(15.3 Å)/Cr(10 Å) sample calculated at $m=1$ is approximately equal to 73% of the experimental one. The difference between the experimental and calculated GMR values has a number of reasons: (i) an assumption of Fe/Cr and Cr/Fe interfaces identity is too rough, (ii) an assumption of the absence of spin asymmetry in Cr is incorrect, (iii) the wavelength region of the maximal MRE values is not achieved, etc. Each of these assumptions requires the corresponding verification.

IV. CONCLUSIONS

We investigated Fe/Cr superlattices with antiferromagnetic ordering of magnetic moments of adjacent Fe layers

and giant magnetoresistance. Optical ellipsometry shows that contribution to $\varepsilon_{\text{eff}}(\omega)$ from free carriers becomes dominating in the wavelength range of $\lambda \geq 8$ μm. We succeeded in obtaining information on magnetotransport properties of electrons at interfaces from magnetoreflection. Relaxation times τ_i and $\tau_i^{\uparrow(\downarrow)}$ and spin asymmetry coefficient of the interface scattering $\gamma_{\text{Fe/Cr(100)}}$ are defined from the MRE spectra in the free carriers region. The value of $\gamma_{\text{Fe/Cr(100)}} = -0.59 \pm 0.04$ agrees well with its theoretical estimation.[33] Probabilities of electron scattering for up-spin and down-spin directions at the Fe/Cr(100) interface are equal to 0.24 for $P_i^{\uparrow}$ and 0.10 for $P_i^{\downarrow}$. In the wavelength range of $\lambda \leq 8$ μm, the MRE reflection spectra of Fe-based materials should not be analyzed in the framework of Jacquet-Valet theory[6] since the effect observed in this spectral region is mainly caused by interband transitions of electrons.

ACKNOWLEDGMENTS

The authors thank M. A. Miljaev for the help in sample preparation. Support by the Russian Foundation for Basic Research under Grant No. RFFI-10-02-00590-a, the fund of the President of the Russian Federation for the support of scientific schools under Grant No. NSH 3545.2010.2, and the Program of the Russian Academy of Science Presidium "The principles of fundamental researches of nanotechnologies and nanomaterials" under Grant No. 27 is gratefully acknowledged.

[1] R. E. Camley and J. Barnas, Phys. Rev. Lett. **63**, 664 (1989).
[2] J. Barnaś, A. Fuss, R. E. Camley, P. Grünberg, and W. Zinn, Phys. Rev. B **42**, 8110 (1990).
[3] P. M. Levy, Solid State Phys., Adv. Res. Appl. **47**, 367 (1994).
[4] V. V. Ustinov, J. Magn. Magn. Mater. **165**, 125 (1997).
[5] M. A. Gijs and E. W. Bauer, Adv. Phys. **46**, 285 (1997).
[6] J. C. Jacquet and T. Valet, in *Magnetic Ultrathin Films, Multilayers and Surfaces*, edited by E. Marinero, MRS Symposia Proceedings No. 384 (Materials Research Society, Pittsburgh, 1995), p. 477.
[7] R. Atkinson, P. M. Dodd, N. F. Kubrakov, A. K. Zvezdin, and K. A. Zvezdin, J. Magn. Magn. Mater. **156**, 169 (1996).
[8] N. F. Kubrakov, A. K. Zvezdin, K. A. Zvezdin, V. A. Kotov, and R. Atkinson, JETP **87**, 600 (1998).
[9] A. B. Granovskii, M. V. Kuz'michev, and J. P. Clerc, JETP **89**, 955 (1999).
[10] V. I. Belotelov, A. K. Zvezdin, V. A. Kotov, and A. P. Pyatakov, Phys. Solid State **45**, 1957 (2003).
[11] J. van Driel, F. R. de Boer, R. Coehoorn, G. H. Rietjens, and E. S. J. Heuvelmans-Wijdenes, Phys. Rev. B **61**, 15321 (2000).
[12] J.-Q. Wang, M. T. Sidney, J. D. Rokitowski, N. H. Kim, and K. Wang, J. Appl. Phys. **103**, 07F316 (2008).
[13] M. Vopsaroiu, D. Bozec, J. A. D. Matthew, S. M. Thompson, C. H. Marrows, and M. Perez, Phys. Rev. B **70**, 214423 (2004).
[14] V. G. Kravets, D. Bozec, J. A. D. Matthew, S. M. Thompson, H. Menard, A. B. Horn, and A. F. Kravets, Phys. Rev. B **65**, 054415 (2002).
[15] I. V. Bykov, E. A. Gan'shina, A. B. Granovskii, and V. S. Gushchin, Phys. Solid State **42**, 498 (2000); A. Granovskii, V. Gushchin, I. Bykov, A. Kozlov, N. Kobayashi, S. Ohnuma, T. Masumoto, and M. Inoue, *ibid.* **45**, 911 (2003).
[16] D. Hrabovský, J. M. Caicedo, G. Herranz, I. C. Infante, F. Sánchez, and J. Fontcuberta, Phys. Rev. B **79**, 052401 (2009); V. G. Kravets, L. V. Poperenko, and A. F. Kravets, *ibid.* **79**, 144409 (2009).
[17] S. Uran, M. Grimsditch, E. E. Fullerton, and S. D. Bader, Phys. Rev. B **57**, 2705 (1998).
[18] V. V. Ustinov, I. D. Lobov, V. M. Maevskii, and L. N. Romashev, in *Proceedings of Moscow International Symposium on Magnetism*, edited by A. Granovskii and N. Perov (Moscow State University, Moscow, 1999), Part 1, p. 333.
[19] V. V. Ustinov, Yu. P. Sukhorukov, M. A. Milyaev, A. B. Granovskii, A. N. Yurasov, E. A. Gan'shina, and A. V. Telegin, JETP **108**, 260 (2009).
[20] I. D. Lobov, M. M. Kirillova, L. N. Romashev, M. A. Milyaev, and V. V. Ustinov, Phys. Solid State **51**, 2480 (2009).
[21] J. R. Beattie, Philos. Mag. **46**, 235 (1955).
[22] V. P. Shirokovskii, M. M. Kirillova, and N. A. Shilkova, Sov. Phys. JETP **55**, 464 (1982).
[23] M. M. Kirillova and L. V. Nomerovannaya, Phys. Met. Metallogr. **40**, 69 (1975).
[24] S. V. Khalilov and Yu. A. Uspenskii, Fiz. Met. Metalloved. **66**, 1097 (1988) (in Russian).
[25] Yu. A. Uspenskii and S. V. Khalilov, Sov. Phys. JETP **68**, 588 (1989).
[26] R. J. Baxter, D. G. Pettifor, E. Y. Tsymbal, D. Bozec, J. A. D. Matthew, and S. M. Thompson, J. Phys.: Condens. Matter **15**, L695 (2003).
[27] R. T. Mennicke, D. Bozec, V. G. Kravets, M. Vopsaroiu, J. A. D. Matthew, and S. M. Thompson, J. Magn. Magn. Mater. **303**, 92 (2006).
[28] T. Valet and A. Fert, Phys. Rev. B **48**, 7099 (1993).
[29] A. B. Drovosekov, N. M. Kreines, M. A. Milyaev, L. N. Romashev, and V. V. Ustinov, J. Magn. Magn. Mater. **290-291**, 157 (2005).
[30] I. D. Lobov, M. M. Kirillova, L. N. Romashev, V. V. Ustinov, V. M. Maevskii, and M. A. Milyaev, J. Magn. Magn. Mater. **300**, e359 (2006).
[31] D. Spišák and J. Hafner, Phys. Rev. B **61**, 4160 (2000).
[32] C. Vouille, A. Fert, A. Barthelemy, S. Y. Hsu, R. Loloee, and P. A. Schroeder, J. Appl. Phys. **81**, 4573 (1997).
[33] M. D. Stiles and D. R. Penn, Phys. Rev. B **61**, 3200 (2000).
[34] J. Schäfer, M. Hoinkis, E. Rotenberg, P. Blaha, and R. Claessen, Phys. Rev. B **72**, 155115 (2005).